# Chapter 21
# Visualization in Connectomics

**Hanspeter Pfister, Verena Kaynig, Charl P. Botha, Stefan Bruckner, Vincent J. Dercksen, Hans-Christian Hege and Jos B.T.M. Roerdink**

**Abstract** Connectomics is a branch of neuroscience that attempts to create a *connectome*, i.e., a complete map of the neuronal system and all connections between neuronal structures. This representation can be used to understand how functional brain states emerge from their underlying anatomical structures and how dysfunction and neuronal diseases arise. We review the current state-of-the-art of visualization and image processing techniques in the field of connectomics and describe a number of challenges. After a brief summary of the biological background and an overview of relevant imaging modalities, we review current techniques to extract connectivity

H. Pfister (✉) · V. Kaynig
School of Engineering and Applied Sciences, Harvard University,
33 Oxford St., Cambridge, MA 02138, USA
e-mail: pfister@seas.harvard.edu

V. Kaynig
e-mail: vkaynig@seas.harvard.edu

C.P. Botha
vxlabs, Somerset West, SA
e-mail: cpbotha@vxlabs.com

S. Bruckner
Institute of Computer Graphics and Algorithms, Vienna University of Technology,
Favoritenstraße 9-11/E186, 1040 Wien, Austria
e-mail: bruckner@cg.tuwien.ac.at

V.J. Dercksen · H.-C. Hege
Department of Visualization and Data Analysis,
Zuse Institute Berlin, Takustraße 7, 14195 Berlin, Germany
e-mail: dercksen@zib.de

H.-C. Hege
e-mail: hege@zib.de

J.B.T.M. Roerdink
Johann Bernoulli Institute for Mathematics and Computer Science,
University of Groningen, P.O. Box 407, 9700, AK Groningen, The Netherlands
e-mail: j.b.t.m.roerdink@rug.nl

information from image data at macro-, meso- and microscales. We also discuss data integration and neural network modeling, as well as the visualization, analysis and comparison of brain networks.

## 21.1 Introduction

Connectomics is a field of neuroscience that analyzes neuronal connections. A connectome is a complete map of a neuronal system, comprising all neuronal connections between its structures. The term 'connectome' is close to the word 'genome' and implies completeness of all neuronal connections, in the same way as a genome is a complete listing of all nucleotide sequences. The goal of connectomics is to create a complete representation of the brain's wiring. Such a representation is believed to increase our understanding of how functional brain states emerge from their underlying anatomical structure [89]. Furthermore, it can provide important information for the cure of neuronal dysfunctions like schizophrenia or autism [83].

Different types of connectivity can be distinguished. *Structural* or anatomical connectivity usually refers to the "wiring diagram" of physical connections between neural elements. These anatomical connections range in scale from those of local circuits of single cells to large-scale networks of interregional pathways [87]. *Functional* connectivity is defined as "the temporal correlation between spatially remote neurophysiological events" [32]. This can be seen as a statistical property; it does not necessarily imply direct anatomical connections. Finally, *effective* connectivity concerns causal interactions between distinct units within a nervous system [32].

Sporns et al. [89] differentiate between macro-, meso- and microscale connectomes. At the *macroscale*, a whole brain can be imaged and divided into anatomically distinct areas that maintain specific patterns of interconnectivity. Spatial resolution at the macroscale is typically in the range of millimeters. One order of magnitude smaller is the *mesoscale* connectome that describes connectivity in the range of micrometers. At this scale, local neuronal circuits, e.g., cortical columns, can be distinguished. At the finest *microscale*, the connectome involves mapping single neuronal cells and their connectivity patterns. Ultimately, connectomes from all scales should be merged into one hierarchical representation [89].

Independently of the scale, the connectivity can be represented as a *brain graph* $G(N; E)$ with nodes $N$ and weighted edges $E$ representing anatomical entities and the degree of structural or functional interactions, respectively. Associated to each abstract graph is a graph in real space that connects real anatomical entities. Neural systems can be investigated by analyzing topological and geometrical properties of these graphs and by comparing them. An equivalent way of representing an undirected or directed brain graph is a *connectivity* or *association matrix C*, whose entries $c_{ij}$ represent the degrees of interactions. Thresholding and sometimes also binarizing them reveals the essential interactions. A spatial connectivity graph can be depicted in real space, showing the actual physical structure of the neural system. A connec-

tion matrix is usually visualized using a color-coded matrix view. For more details and examples see, e.g., the recent reviews [12, 30].

In contrast to genomics, the field of connectomics is to a large extent based on image data. Therefore, visualization of image data can directly support the analysis of brain structures and their structural or functional connections.

In this chapter, we review the current state-of-the-art in visualization and image processing techniques in the field of connectomics and describe some remaining challenges. After presenting some biological background in Sect. 21.2 and an overview of relevant imaging modalities in Sect. 21.3, we review current techniques to extract connectivity information from image data at macro-, meso- and microscale in Sects. 21.4–21.6. Section 21.7 focuses on integration of anatomical connectivity data. The last section discusses visually supported analysis of brain networks.

## 21.2 Biological Background

**Neural systems**. Functionally, neurons (or nerve cells) are the elementary signaling units of the nervous system, including the brain. Each neuron is composed of a cell body (soma), multiple dendritic branches and one axonal tree, which receive input from and transfer output towards other neurons, respectively. This transfer is either chemical (synapses) or electrical (gap junctions). Generally, during synaptic transmission, vesicles containing neurotransmitter molecules are released from terminals (boutons) on the axon of the presynaptic neuron, diffuse across the synaptic cleft, and are bound by receptors on dendritic spines of the postsynaptic neuron, inducing a voltage change, i.e., a signal.

These basic building blocks can mediate complex behavior, as potentially large numbers of them are interconnected to form local and long-range neural microcircuits. At the meso-level, local neuron populations, e.g., *cortical minicolumns*, can be identified that act as elementary processing units. At the macroscale, neurons in the human cortex are arranged in a number of anatomically distinct areas, connected by interregional pathways called *tracts* [89].

**Model systems**. An important neuroscientific goal is to understand how the human brain works. However, due to its complexity (with an estimated $10^{11}$ neurons with $10^{15}$ connections [89]), brain function at the circuit or cellular level is often studied in other organisms that are more amenable in complexity and size.

Conserved genes and pathways between different species offer the potential of elucidating the mechanisms that affect complex human traits based on similar processes in other organisms. This problem is particularly tractable in the roundworm *Caenorhabditis elegans*, whose brain with 302 neurons has been completely mapped [106], or in insects. In these organisms brain structure and function can be studied at the level of single identifiable neurons. Classical insect model organisms that are well understood and allow easy genetic manipulations are the fruit fly *Drosophila melanogaster* and the honeybee. Drosophila, for example, has been

shown to be an experimentally amenable model system even for the study of such quintessential human physiological traits as alcoholism, drug abuse, and sleep [63].

Rodents, being mammals, have a brain structure that is similar but much smaller than the human brain, and that therefore can be used to study cortical networks. The mouse brain is an attractive model system to study, for example, the visual system, due to the abundant availability of genetic tools allowing monitoring and manipulating certain cell types or circuits [38]. The whisker-barrel pathway of the rat is a relatively small and segregated circuit that is amenable to studying sensory information processing at the molecular/synaptic, cell, and circuit/region levels.

## 21.3 Imaging Modalities Employed in Connectomics

We now provide an overview of imaging modalities that are used in obtaining connectivity information. They differ in the spatial and temporal resolution at which connectivity is captured. At the *macroscale* there is a wide range of structural and functional imaging modalities, with applications in medical settings and anatomical research. Functional imaging modalities include electroencephalography (EEG), magnetoencephalography (MEG), functional magnetic resonance imaging (fMRI), and positron emission tomography (PET). Modalities such as single-photon emission computed tomography (SPECT) and magnetic resonance imaging (MRI) provide structural information on the macroscale. Section 21.4 gives a detailed introduction to the relevant modalities in the context of connectomics. At the *mesoscale*, light microscopy (LM) techniques provide sufficient resolution to image single neurons. Most light microscopy techniques focus on structural imaging. Techniques such as wide-field fluorescence microscopy allow for the imaging of living cells, and computational optical sectioning microscopy techniques [17] enable non-destructive acquisition of 3D data sets. Section 21.5 provides further details about light microscopy techniques. At the *microscale*, the sufficient resolution is offered by electron microscopy techniques (EM) such as Transmission Electron Microscopy (TEM) and Scanning Electron Microscopy (SEM). These methods require technically complex specimen preparation and are not applicable to live cell imaging. Imaging of 3D volumes requires ultra-thin sectioning of the brain tissue followed by computational realignment of the acquired images into one image volume [46]. More information about electron microscopy in the connectomics setting can be found in Sect. 21.6. Figure 21.1 provides an overview of the different imaging modalities and their spatial and temporal resolution.

## 21.4 Macroscale Connectivity

First, we discuss the main acquisition techniques for revealing macroscopic functional and structural connectivity. We start with MEG and EEG, as these were used for functional connectivity before fMRI, then diffusion-weighted MRI for structural
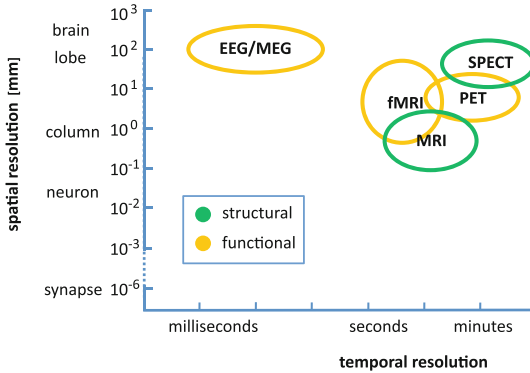
**Fig. 21.1** Different brain imaging modalities and their spatial and temporal resolutions. For connectomics, light-(*LM*) and electron microscopy (*EM*) are mostly performed in vitro. The color indicates functional versus structural information in the acquired data

connectivity, and finally fMRI for functional connectivity. Besides the visualization approaches discussed here, the reader is also referred to Sect. 21.8 for more detail on network analysis and comparative visualization techniques.

### 21.4.1 EEG and MEG

Developed in the 1920s, electroencephalography (EEG) is the oldest noninvasive functional neuroimaging technique, which records electrical brain activity from electrodes on the scalp. Nowadays, the number of electrodes can be as large as 128 or even 512; in that case one speaks of *multichannel* or *high-density* EEG [81, 93]. By contrast, magnetoencephalography (MEG) measures magnetic fields outside the head induced by electrical brain activity [35]. The temporal frequency of these signals ranges from less than 1 Hz to over 100 Hz. The spatial resolution is lower than that of fMRI. Sometimes, MEG is preferred over EEG because the electrical signals measured by EEG depend on the conduction through different tissues (e.g., skull and skin). However, EEG has much lower costs and higher equipment transportability than MEG (and fMRI). Moreover, EEG allows participants more freedom to move than MEG and fMRI. In Sect. 21.8 we will discuss the use of EEG to discover functional brain networks. Therefore, we will focus on EEG for the remainder of this section.

Electrical potentials generated within the brain can be measured with electrodes at the scalp during an EEG recording. The measured EEG signals reflect rhythmical activity varying with brain state. Specific brain responses can be elicited by the presentation of external stimuli. For EEG analysis, one often studies activity in various frequency bands, such as alpha, beta, theta or delta bands. As a result of *volume conduction*, an electrical current flows from the generator in the brain through different

tissues (e.g., brain, skull, skin) to a recording electrode on the scalp. The measured EEG is mainly generated by neuronal (inhibitory and excitatory) postsynaptic potentials and burst firing in the cerebral cortex. Measured potentials depend on the source intensity, its distance from the electrodes, and on the conductive properties of the tissues between the source and the recording electrode.

Several visualization methods are applied to assist in the interpretation of the EEG [93]. In a conventional EEG visualization, the time-varying EEG data are represented by one time series per electrode, displaying the measured potential as a function of time. Synchronous activity between brain regions is associated with a functional relationship between those regions. EEG coherence, calculated between pairs of electrode signals as a function of frequency, is a measure for this synchrony. A common visualization of EEG coherence is a graph layout. In the case of EEG, graph vertices (drawn as dots) represent electrodes and graph edges (drawn as lines between dots) represent similarities between pairs of electrode signals. Traditional visual representations are, however, not tailored for multichannel EEG, leading to cluttered representations. Solutions to this problem are discussed in Sect. 21.8.

## 21.4.2 MRI

In magnetic resonance imaging, or MRI, unpaired protons, mostly in hydrogen atoms, precess at a frequency related to the strength of the magnetic field applied by the scanner. When a radio-frequency pulse with that specific frequency is applied, the protons resonate, temporarily changing their precession angle. They eventually regain their default precession angle, an occurrence that is measured by the scanner as an electromagnetic signal. By applying magnetic field gradients throughout three-dimensional space, protons at different positions will precess and hence resonate at different frequencies, enabling MRI to generate volume data describing the subject being scanned.

### 21.4.2.1 Diffusion-Weighted Imaging

Water molecules at any temperature above absolute zero undergo Brownian motion or molecular diffusion [23]. In free water, this motion is completely random, and water molecules move with equal probability in all directions. In the presence of constraining structures such as the axons connecting neurons together, water molecules move more often in the same direction than they do across these structures. When such a molecule moves, the two precessing protons its hydrogen nucleus contains move as well. When this motion occurs in the same direction as the diffusion gradient $q$ (an extra magnetic field gradient that is applied during scanning) of a diffusion-weighted MRI scan, the detected signal from that position is weakened. By applying diffusion gradients in a number of different directions, a dataset can be

built up showing the 3D water diffusion at all points in the volume, which in turn is related to the directed structures running through those points.

**Diffusion tensor imaging.** When at least six directions are acquired, a $3 \times 3$ symmetric diffusion tensor can be derived, in which case the modality is described as Diffusion Tensor Imaging (DTI). Per voxel DTI, often visualized with an ellipsoid, is not able to represent more than one major diffusion direction through a voxel. If two or more neural fibers were to cross, normal single tensor DTI would show either planar or more spherical diffusion at that point. The left image of Fig. 21.2 shows a 3-D subset of such a dataset, where each tensor has been represented with a superquadric glyph [50].

DTI visualization techniques can be grouped into the following three classes [102]: *Scalar metrics* reduce the multi-valued tensor data to one or more scalar values such as fractional anisotropy (FA), a measure of anisotropy based on the eigenvalues of the tensor, and then display the reduced data using traditional techniques, for example multi-planar reformation (slicing) or volume rendering. An often-used technique is to map the FA to intensity and the direction of the principal tensor eigenvector to color and then display these on a slice. Multiple anisotropy indices can also be used to define a transfer function for volume rendering, which is then able to represent the anisotropy and shape of the diffusion tensors [49].

*Glyphs* can be used to represent diffusion tensors without reducing the dimensionality of the tensor. In its simplest form, the eigensystem of the tensor is mapped directly to an ellipsoid. More information can be visually represented by mapping diffusion tensors to superquadrics [50] (see Fig. 21.2).

*Vector- and tensor-field visualization* techniques visualize global information of the field. The best known is probably fiber tractography, where lines are reconstructed that follow the tensor data in some way and hence are related to the major directions of neural fibers. In its simplest form, streamlines, tangent to the principal eigenvec-
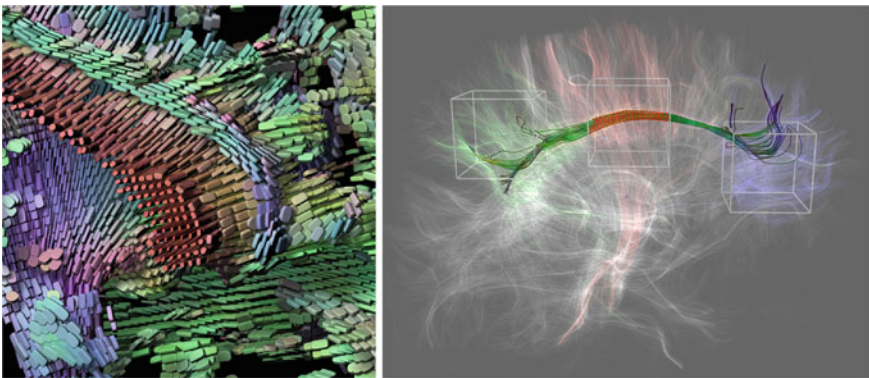


**Fig. 21.2** *On the left*, superquadric glyphs have been used to represent the diffusion tensors in a 3-D region of a brain dataset (image courtesy of Gordon Kindlmann, University of Chicago). *On the right*, the cingulum neural fiber bundle has been highlighted in a full-brain tractography [8]

tors of the diffusion tensors, are extracted and displayed [2]. Care must to be taken to terminate the streamlines in areas of isotropic or planar diffusion. Hyperstreamlines take into account more of the tensor information [109]. Many tractography approaches require one or more regions of interest to be selected *before* tracts can be seeded starting only from those regions, while more recent efforts allow for full-brain fiber tracking followed by more intuitive interactive selection within the brain's tracked fiber bundles [8, 85] (see the right image in Fig. 21.2 for an example). For a simplified visual representation, the envelopes of clustered streamline bundles can be shown [25], or illustrative techniques such as depth-dependent halos can be used [26]. With probabilistic tractography, local probability density functions of diffusion or connectivity are estimated and can in turn be used to estimate the global connectivity, that is, the probability that two points in the brain are structurally connected [4]. This type of data is arguably a higher fidelity representation of structural connectivity. Connectivity between two points can be visualized with, e.g., constant-probability isosurfaces, with direct volume rendering of the probability field, or using topological methods from flow visualization [82]. Calculating and effectively visualizing a full-brain probabilistic tractography would be challenging.

**DSI and HARDI.** As explained above, DTI is not able to capture more than one principal direction per sample point. In order to reconstruct the full diffusion probability density function (PDF), that is, the function describing the probability of water diffusion from each voxel to all possible displacements in the volume, about 500 or more diffusion-weighted MRI volumes need to be acquired successively. This is called diffusion spectrum imaging or DSI [34] and is the canonical way of acquiring the complete 3-D water diffusion behavior. However, the time and processing required to perform full DSI complicate its use in research and practice.

In High Angular Resolution Diffusion Imaging, or HARDI, 40 or more directions are typically acquired in order to sample the 3-D diffusion profile around every point [95]. Based on such data, multiple diffusion tensors can be fit to the data [95], higher order tensors can be used [69], or a model-free method such as Q-Ball imaging [96] can be applied. Q-Ball yields as output an orientation distribution function, or ODF. The ODF is related to the diffusion PDF in that it describes for each direction the sum of the PDF values in that direction. It can be visualized as a deformed sphere whose radii represent the amount of diffusion in the respective direction.

HARDI visualization follows much the same lines as DTI visualization, except that the data are more complex. Analogous to DTI, HARDI scalar metrics, such as generalized (fractional) anisotropy and fractional multifiber index, can be used to reduce the data to one or more scalar values that can be visualized with traditional techniques. Multiple diffusion tensors can be represented as glyphs, or the diffusion ODF can be directly represented using a tessellated icosahedron or by raycasting the spherical harmonics describing the ODF [70]. This results in a field of complex glyphs representing at each point the diffusion profile at that position. In contrast to DTI glyph techniques, regions of crossing fibers can in general be identified.

Although there are fewer examples, especially in the visualization literature, (probabilistic) fiber tracking can be performed based on HARDI data [72]. More

recently, HARDI glyphs have been combined dynamically with DTI glyphs and fiber tracts based on local data characteristics [73].

### 21.4.3 Functional MRI

Blood-oxygen-level dependence, or BOLD, is a special type of MRI that is able to measure increased levels of blood oxygenation [67]. Due to requiring more glucose from the bloodstream, active neurons cause higher blood oxygenation in nearby veins. Based on this principle, functional MRI, or fMRI, uses BOLD to image time-dependent 3-D neural activity in the brain [68].

fMRI can also be used to derive functional or *effective connectivity* in the brain. Functional connectivity is determined by calculating the temporal correlations between the fMRI signals originating from different parts of the brain [32]. This is done either whilst the subject performs a specific task, in order to assess how the brain network is applied during that task, or during resting state, in order to derive the baseline functional brain network. Connectivity data can be determined between a specific seed region or voxel and one or more other regions or voxels, or exhaustively between all regions or voxels in the brain.

Effective connectivity, defined as the causal influence one neuronal system exerts over another, is dependent on a model of the connectivity between the participating regions. For example, the signal at one position could be expressed as the weighted sum of the signals elsewhere [32]. If the model is invalid, the effective connectivity derived from fMRI is also invalid.

Visualization of fMRI-derived connectivity information is quite varied, often combining techniques from scientific and information visualization. Scatter plots have been used to plot correlation strength over distance, dendrograms and multi-dimensional scaling to represent correlations between regions in 2D [80], matrix bitmaps to represent region-wise correlation matrices [28], 2-D and 3-D (pseudo-) anatomical node-link diagrams to show the derived brain networks [107], and coupled-view visual analysis techniques to explore resting state fMRI data [99]. When connectivity is determined between all pairs of voxels in the cortex, visualization and knowledge extraction pose perceptual and computational challenges that have not yet been fully explored.

## 21.5 Mesoscale Connectivity

Light microscopy was the first modality that allowed for imaging of single neuronal cells. While the resolution of a light microscope is not sufficient to resolve synapses, it allows for the identification of major cell parts, such as dendrites, somas, axons, and also boutons as possible locations for synaptic connections. Imaging whole neuronal cells and analyzing their geometry enables neuroanatomists to identify different types

of cells and to come to conclusions about their function. Following the motto "the gain in the brain lies mainly in the stain" [1], the three following main techniques are employed to map neuronal circuits with light microscopy [60].

**Single-cell staining by dye impregnation.** This is the oldest staining method and it laid the foundation for modern neuroscience. As neuronal tissue is densely packed with cells, a complete staining of the whole sample would not allow one to discriminate single cells in light microscopy images. Instead, the so-called *Golgi stain* enables stochastic marking of just a few individual nerve cells. The stained cells appear dark in the light microscopy images, discriminating them from a bright background formed by the unstained tissue. This staining method, combined with the ability of the light microscope to focus on different depth of the sample, allows for 3D imaging of the cell geometry. The famous neuroscientist Cajal (1852–1934) was able to identify different types of neurons and also describe connectivity patterns and principles of neuronal circuit organization using Golgi's method [60].

**Diffusion or transport staining.** Diffusion staining techniques enable biologists to analyze the projective trajectory of brain regions. For this technique, different staining markers are injected into different regions of the brain *in vivo*. The staining is then diffused along the connected neurons. Finally, a sample of brain tissue is extracted from a different region, in which no marker has been injected. The color code in the staining of different neurons in this area then reveals the projection of these neurons back to the initial staining areas, providing information about long-distance connectivity [33]. The range of possible colors for this method is limited to three or four different stainings.

**Multicolor or brainbow.** This staining technique does not involve application or injection of staining to brain tissue. Instead, transgenic mice are bred to produce photophysical fluorescent proteins. A confocal laser-scanning microscope activates the fluorescent proteins with a laser beam and records an image with the expressed light. Brainbow mice are bred to express three fluorescent proteins of different colors. By different stochastic expression of these three colors, the single neurons of the mice are colored with one out of >100 labels. The main advantage of this method is that it allows one to uniquely identify dendrites and axons belonging to the same neuron in densely colored tissue [60], see also Fig. 21.3.

All of these three staining methods allow imaging the geometry of neurons at the micrometer scale. The different staining protocols all aim at visually separating single neurons out of the complex and dense neuronal tissue. Visualization techniques for connectomics need to enhance the visual separation further, e.g., by providing contrast enhancement and enabling flexible mappings of image data to varying amounts of transparency in the transfer function [51]. Especially for the brainbow staining it is useful to have visual enhancement of color differences in regions of interest where two neurons with a similar staining combination need to be distinguished. For diffusion staining this problem is less pronounced than for brainbow data, as typically only three to four easily distinguishable colors are used. But this also leads to the challenge of distinguishing two neighboring cells that are

**Fig. 21.3** Brainbow image of mouse cerebral cortex tissue. The different color stainings facilitate the differentiation of neuronal cells. Image courtesy of Jean Livet and Jeff Lichtman
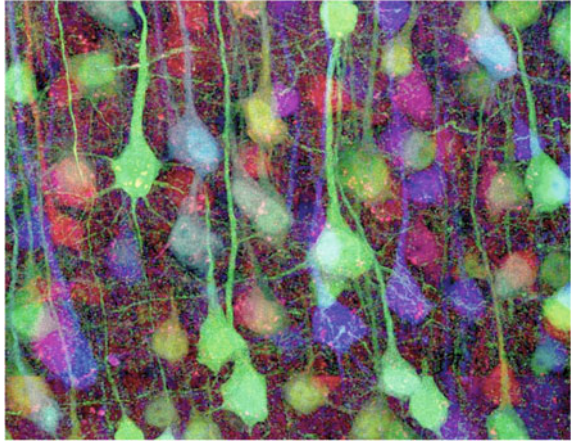
stained with the same color. This problem also arises in the Golgi stain, as only one color is applicable for this staining. Thus, visualization needs to focus on providing a good impression of the neurons' geometry. The user needs to be able to access the three-dimensional structure on different scale levels to infer the connectivity of dendritic parts and axons. In order to analyze the neuron geometry further, dendritic and axonal trees have to be identified and segmented. This task is typically performed either semi-automatically or fully automatically with a final proof-reading step [97].

An additional major challenge for the visualization of microscopy data sets in the field of connectomics is the large data volume required to analyze the geometry of full neurons. Microscopes typically only record regions of interest at the required resolution. Afterwards the acquired images or image stacks need to be stitched into one large data volume. While this problem is well known and automatic methods for image stitching and alignment exist [24, 74], these tools typically work offline, assembling all images into one large image file for later visualization. But with image volumes in the gigapixel range this method is no longer applicable. Instead, visualization tools are required to perform operations like image stitching, alignment, contrast enhancement, and denoising *on-demand* in the region of interest shown to the user. To allow for interactive visualization, these operations do not only need to be executed fast, but also on multiple scales, allowing the user to zoom in and out of the displayed data volume. Recent work by Jeong et al. [41] provides this demand-driven visualization approach and combines it with a client server architecture. The client can visualize the data with user interaction and annotation while computations are performed on a high-performance server transparently to the user. Multiple client instances can connect to the same server to allow multiple users to access the data at the same time and cooperatively work on the same data set.

## 21.6 Microscale Connectivity

In contrast to light microscopy, which is limited in its resolution by the wavelength of light, electron microscopy enables imaging of neuronal tissue at the nanometer scale. Hence, electron microscopy is the only imaging modality so far that can resolve single synapses. However, the sample preparation and image acquisition in electron microscopy is labor-intensive and time-consuming. As a consequence, the analysis of the connectivity between single neurons has been limited to sparse analysis of statistical properties such as average synapse densities in different brain regions [20]. Little is known about the complete connectivity between single neurons. Information about the individual strength of synapses or the number of connections between two cells can have important implications for computational neuroanatomy and theoretical analysis of neuronal networks [98].

Recently, significant progress has been made in the automation of ultra-thin serial sectioning [36] and automatic image acquisition [21, 52]. These techniques allow neuroanatomists to acquire large datasets of multiple terabytes (TB) in size. With a resolution of 5 nm per pixel, and a section thickness of 50 nm, one cubic millimeter of brain tissue requires imaging of 20,000 sections with 40 gigapixels per image, leading to an image volume of 800 TB. With data sets of this size new challenges emerge for automatic computed analysis and visualization techniques. Important processing tasks include demand-driven image stitching and alignment, cell segmentation and 3D reconstruction, as well as multi-scale visualization and multi-user interaction via client server architectures.

Electron microscopy samples are typically densely stained. While in light microscopy sparse staining is necessary to visually separate a cell of interest from unstained background tissue (see Sect. 21.5), the fine resolution of electron microscopy allows one to discriminate structures according to shape, size, and texture. Electron microscopy images are limited to gray scale and typically do not have a uniform background. Instead, the background is noisy and highly variable, which imposes an important challenge for the visualization of electron microscopy image stacks. The image data cannot be visualized according to gray values alone, as the densely stained tissue forms a nearly solid block. Instead, higher order features that discriminate texture and shape, e.g., gradient histograms, are necessary to enhance the visibility of different structures of interest in the visualization [42]. Ultimately, full segmentation of the image data is necessary to allow the user visual inspection of different biological structures, from small structures such as vesicles or mitochondria to entire neuronal cells. Figure 21.4 shows example reconstructions of different neuronal structures from electron microscopy images. A number of software packages have been developed to aid the user in manual segmentation of cell structures in the images [14, 29, 37]. More recent semi-automatic methods greatly facilitate this time-intensive process [16, 76, 77, 91].

Progress has also been made on fully automatic segmentation of EM brain images [39, 44, 47, 48, 101, 103]. However, all methods developed so far require manual interaction and inspection by users. Thus, visualization tools should not only provide the ability to inspect the original EM data and the computed segmentations, but also
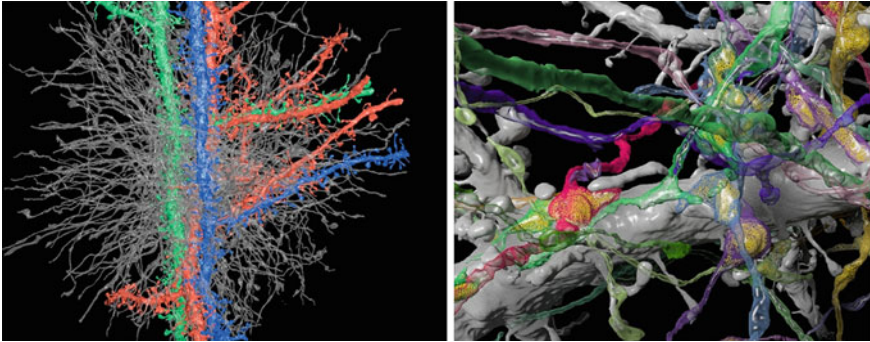
**Fig. 21.4** Three dimensional reconstructions of neuronal structures from electron microscopy data. *Left* three dendrites (colored) and all intervening axons (transparent), *right* different axons (colored) with vesicle filled boutons (*yellow*)

provide a user interface to detect and correct segmentation errors, a process called *proofreading*.

Another interesting challenge for the visualization of neuronal microscopy images is the concurrent display of light and electron microscopy data acquired from the same sample. Correlative microscopy is a newly developing field, which allows for inspection of the same neuronal tissue using both light and electron microscopes. Thus the fine resolution of the electron microscopy images can be combined with the advantage of color staining and information about long-range connectivity in, e.g., diffusion stained light microscopy images. Visualization of this data requires multi-modal registration of both data sets, which has not yet been addressed for correlative microscopy.

Currently, most research efforts in connectomics at the microscale concentrate on the image acquisition and segmentation of electron microscopy images. Little research has been done in the visualization of entire connectomes, i.e. the wiring diagram of neurons, their types and the connectivity for detailed analysis of neuronal circuits. Connectomes, like the manually reconstructed circuit of C. elegans, are visualized by connectivity matrices or connection graphs [100].

## 21.7 Data Integration and Neural Network Modeling

As described in the previous sections, neurobiological data can be acquired from many different sources. Relating these different kinds of data by integrating them in a common reference frame offers interesting opportunities to infer new knowledge about the relation between structure and function. In this section, we describe two approaches and their visualization aspects for such data integration with the purpose of inferring functional properties: brain mapping and network modeling by reverse engineering.

### *21.7.1 Brain Mapping*

A major goal in neuroscience is to define the cellular architecture of the brain. Mapping the fine anatomy of complex neuronal circuits is an essential first step in investigating the neural mechanisms of information processing. The term *brain mapping* describes a set of neuroscience techniques predicated on the mapping of biological quantities or properties onto spatial representations of the brain resulting in maps. While all of neuroimaging can be considered part of brain mapping, the term more specifically refers to the generation of atlases, i.e., databases that combine imaging data with additional information in order to infer functional information. Such an undertaking relies on research and development in image acquisition, representation, analysis, visualization, and interaction. Intuitive and efficient visualization is important at all intermediate steps in such projects. Proper visualization tools are indispensable for quality control (e.g., identification of acquisition artifacts and misclassifications), the sharing of generated resources among a network of collaborators, or the setup and validation of an automated analysis pipeline. Data acquired to study brain structure captures information on the brain at different scales (e.g., molecular, cellular, circuitry, system, behavior), with different focus (e.g., anatomy, metabolism, function), and is multi-modal (text, graphics, 2D and 3D images, audio, video) [15, 53]. The establishment of spatial relationships between initially unrelated images and information is a fundamental step towards the exploitation of available data [7]. These relationships provide the basis for the visual representation of a data collection and the generation of further knowledge.

**Databases and atlases.** A neuroanatomical atlas serves as a reference frame for comparing and integrating data from different biological experiments. Maye et al. [64] give an introduction and survey on the integration and visualization of neural structures in brain atlases. Such atlases are an invaluable reference in efforts to compile a comprehensive set of anatomical and functional data, and in formulating hypotheses on the operation of specific neuronal circuits.

A classical image-based neuroanatomical atlas of Drosophila is the FlyBrain atlas,[1] spatially relating a collection of 2D drawings, microscopic images, and text. One approach in generating a digital atlas of this kind is by acquiring confocal microscope images of a large number of individual brains. In each specimen, one or more distinct neuronal types are highlighted using appropriate molecular genetic techniques. Additionally, a general staining is applied to reveal the overall structure of the brain, providing a reference for non-rigid registration to a standard template. After registration, the specific neuronal types in each specimen are segmented, annotated, and compiled into a database linked to the physical structure of the brain. Jenett et al. [40] describe techniques for quantitative assessment, comparison, and presentation of 3D confocal microscopy images of Drosophila brains and gene expression patterns within these brains. Pereanu and Hartenstein [71] and Rybak et al. [79] described 3D atlases of the developing Drosophila brain and the honeybee brain.

---

[1] http://flybrain.neurobio.arizona.edu

The Neuroterrain 3D mouse brain atlas [5] consists of segmented 3D structures represented as geometry and references a large collection of normalized 3D confocal images.

**Visual exploration and analysis.** 3D microscopy data is often visualized using Maximum Intensity Projection (MIP), which displays the maximum values along viewing rays. Direct Volume Rendering (DVR) enables better perception of spatial relationships, but has the disadvantage of added complexity, as an additional transfer function is required. It can lead to problems with occlusions, particularly when multiple channels need to be visualized simultaneously. Maximum Intensity Difference Accumulation (MIDA) [9] improves this situation by combining the simplicity of MIP with additional spatial cues provided by DVR. Wan et al.[105] presented a tool for the visualization of multi-channel data tailored to the needs of neurobiologists. As acquired volumetric data is typically visualized together with segmented structures, it is important to avoid occlusions as well as visual clutter. Kuß et al. [56] proposed and evaluated several techniques to make spatial relationships more apparent.

However, to enable the exploration of large-scale collections of neuroanatomical data, massive sets of data must be presented in a way that enables them to be browsed, analyzed, queried and compared. An overview of a processing and visualization pipeline for large collections of 3D microscopy images is provided in a study by de Leeuw et al. [59]. NeuARt II [13] provides a general 2D visual interface to 3D neuroanatomical atlases including interactive visual browsing by stereotactic coordinate navigation. Brain Explorer [58], an interface to the Allen Brain Atlas, allows the visualization of mouse brain gene expression data in 3D. The CoCoMac-3D Viewer developed by Bezgin et al. [6] implements a visual interface to two databases containing morphology and connectivity data of the macaque brain for analysis and quantification of connectivity data. An example of an interface to neuroanatomical image collections and databases that features basic visual query functionalities is the European Computerized Human Brain Database (ECHBD) [31]. It connects a conventional database with an infrastructure for direct queries on raster data. Visual queries on image contents can be performed by interactive definition of a volume of interest in a 3D reference image. Press et al. [75] focused on the graphical search within neuroanatomical atlases. Their system, called XANAT, allows for the study, analysis, and storage of neuroanatomical connections. Users perform searches by graphically defining a region of interest to display the connectivity information for this region. Furthermore, their system also supports textual search using keywords describing a particular region. Kuß et al. [55] proposed ontology-based high-level queries in a database of bee brain images based on pre-generated 3D representations of atlas information. In the BrainGazer system [9] anatomical structures can be visually mined based on their spatial location, neighborhood, and overlap with other structures. By delineating staining patterns in a volume rendered image, for example, the database can be searched for known anatomical objects in nearby locations (see Fig. 21.5). Lin et al. [61] presented an approach to explore neuronal structures forming pathways and circuits using connectivity queries. In order to explore the similarity and differences of a large population of anatomical variations, Joshi et
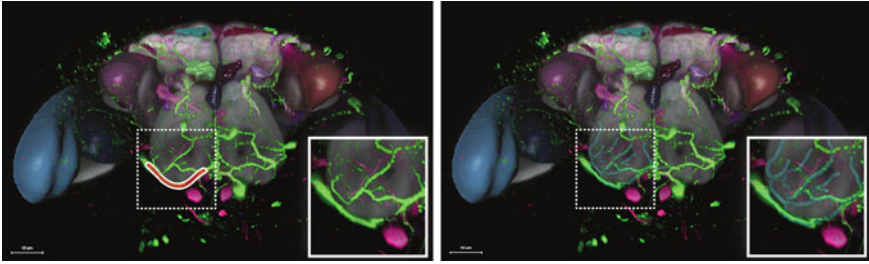
**Fig. 21.5** Visual query for neural projection in the Drosophila brain using the BrainGazer system [9]. *Left* The query is specified by sketching a path on *top* of a Gal4 expression pattern. *Right* An existing segmented neural projection that matches the query is displayed

al. [43] proposed a similarity-space approach that embeds individual shapes in a meta-space for content-driven navigation.

While these efforts represent promising directions, many challenges remain. As noted by Walter et al. [104], a major goal is the integration of brain mapping data with other resources such as molecular sequences, structures, pathways and regulatory networks, tissue physiology and micromorphology. The ever-growing amount of data means that distributed solutions are required. The integration of computational and human resources gives significant benefits: each involved partner may bring computational resources (in terms of hardware and tools), human resources (in terms of expertise), and data to analyze. Advances in web technology, such as HTML5 and WebGL, provide new opportunities for visualization researchers to make their work accessible to the neuroscience community.

### 21.7.2 Neural Network Modeling

A complete reconstruction of the connectivity at the synapse level is currently possible for small brain volumes using electron microscopy techniques, but not yet feasible for volumes the size of a cortical column. Oberlaender et al. [65] therefore pursue a reverse engineering approach: A computational model of a cortical column in the rat somatosensory cortex, consisting of ∼18,000 neurons, is created by integration of anatomical data acquired by different imaging and reconstruction techniques into a common reference system. As the data is acquired from different animals in a population, the network represents an "average" cortical column: some model parameters are given as probabilistic densities. By generating realizations of these stochastic parameters, concrete network models are created.

The number of neurons and their distribution in a cortical column is obtained by automatic counting of neural soma (cell bodies) in confocal images [66]. The 3D dendritic morphologies of ∼100 neurons of different cell types in the column as well as axons are reconstructed from transmitted light bright field images [22]. The column model is created by generating soma positions satisfying the given neuron
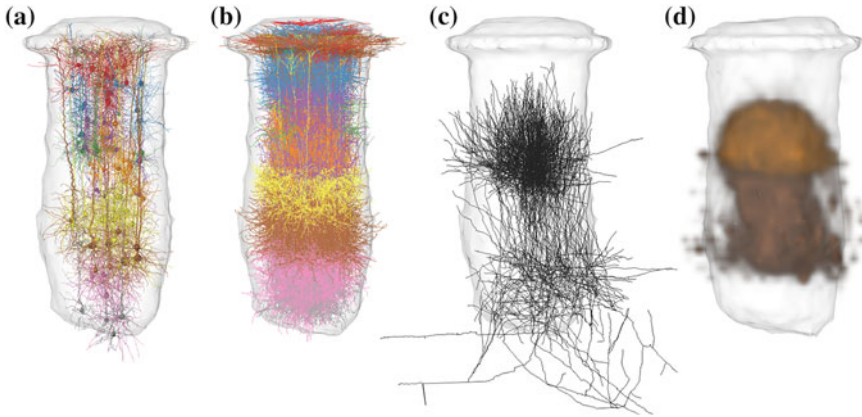
**Fig. 21.6** Reverse engineering of a cortical column. Reconstructed dendrites (**a**) are replicated and inserted into the column reference frame according to a given neuron density (**b**). By determining the local structural overlap with axons projecting into the column (**c**), the number of synapses for different post-synaptic cell types can be estimated. (**d**) Shown are synapse densities for two cell types. Figure created from data published in [65]

density and replicating and inserting the dendrite morphologies into the reference frame according to the given cell type frequency (see Fig. 21.6). Differences in synaptic densities between cell types can be quantified and visualized [65]. Based on the estimated number of synapses per cell, a complete network wiring is established to study network function using numerical simulation [57].

Extracting relevant neurobiological knowledge from such network models is a challenging task. Whereas computation of specific quantities for comparison with literature results in order to validate the model is straightforward, exploratory knowledge discovery within such large, complex networks is not. Easy-to-use tools are needed to let the neurobiologist query and visualize the structural and functional properties of such networks or ensembles of network realizations. As network models are increasing in size, large data handling will be a challenging issue as well.

## 21.8 Network Analysis and Comparative Visualization

A recent innovation in neuroimaging is connectivity analysis, in which the anatomical or functional relation between different (underlying) brain areas is calculated from data obtained by various modalities, allowing researchers to study the resulting *networks* of interrelated brain regions. Of particular interest are *comparisons* of functional brain networks under different experimental conditions and between groups of subjects.

### 21.8.1 Network Measures

For each of the brain connectivity types (anatomical, functional, effective), one can extract networks from data obtained by an appropriate brain imaging modality [10, 54]. The next step is to characterize such networks. In the last decade, a multitude of *topological* network measures have been developed in an attempt to characterize and compare brain networks [11, 45, 78, 90]. Such measures characterize aspects of global, regional, and local brain connectivity.[2] Examples of global measures are characteristic path length, clustering coefficient, modularity, centrality, degree distribution, etc. Some of them, such as clustering coefficient or modularity, refer to *functional segregation* in the brain, i.e., the ability for specialized processing to occur in densely interconnected groups of brain regions. Others characterize *functional integration*, i.e., the ability to rapidly combine specialized information from distributed brain regions [78, 90]. Typical measures in this class are based on the concept of paths in the network, e.g., characteristic path length or global efficiency (average inverse shortest path length). It is believed that both anatomical and functional brain connectivity exhibit *small-world properties*, i.e., they combine functionally segregated modules with a robust number of intermodular links [3, 88]. The degree distribution can be used as a measure of network resilience, i.e., the capacity of the network to withstand network deterioration due to lesions or strokes.

For characterizing networks on a local scale one uses single node features such as in-degree and out-degree, or the local clustering coefficient. Typical regional network measures are *network motifs*, which are defined as patterns of local connectivity. A typical motif in a directed network is a triangle, consisting of feedforward and/or feedback loops. Both anatomical and functional motifs are distinguished. The significance of a certain motif in a network is determined by its frequency of occurrence, and the frequency of occurrence of different motifs around a node is known as the motif fingerprint of that node.

### 21.8.2 Brain Network Comparison and Visualization

The comparison of different brain networks presents challenging problems. Usually the networks differ in number and position of nodes and links, and a direct comparison is therefore difficult. One possible approach is to compute a network measure for each of the networks, and then compare the network measures. However, this loses spatial information. For interpretation and diagnosis it may be essential that local differences can be visualized in the original network representation [27, 86]. This asks for the development of mathematical methods, algorithms and visualization tools for the *local comparison* of complex networks—not necessarily of the same size—obtained under different conditions (time, frequency, scale) or pertaining to different (groups of) subjects.

---

[2] Similar approaches have been used in genomics [62, 84] and other areas.
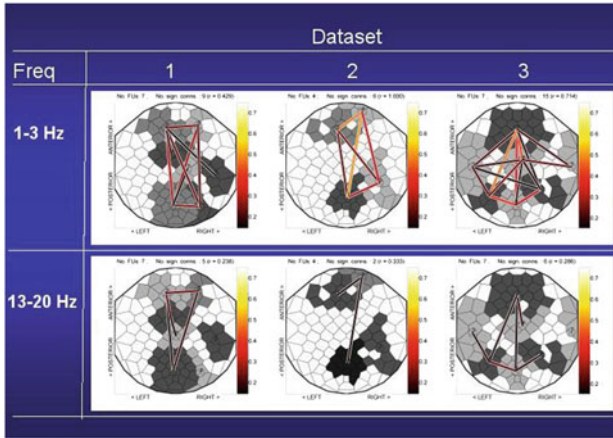
**Fig. 21.7** FU maps for multichannel EEG coherence visualization. Brain responses were collected from three subjects using an EEG cap with 119 scalp electrodes. During a so-called P300 experiment, each participant was instructed to count target tones of 2,000 Hz (probability 0.15), alternated with standard tones of 1,000 Hz (probability 0.85) which were to be ignored. After the experiment, the participant had to report the number of perceived target tones. Shown are FU maps for target stimuli data, with FUs larger than 5 cells, for the 1-3Hz EEG frequency band (*top row*) and for 13–20 Hz (*bottom row*), for three datasets (Figure adapted from [92], Fig. 3)

Several methods exist for spatial comparison of brain networks, which assume that the position and number of network nodes is the same in the networks to be compared. For example, Salvador et al. [80] use a brain parcellation based on a prior standard anatomical template, dividing each cerebral hemisphere into 45 anatomical regions that correspond to the nodes of the brain network. Another possibility is to consider each voxel a network node, but in this way the networks become very large. Links between the nodes can then be defined by several measures of node-node association, such as correlation or mutual information of temporal signals. Using the same construction for two or more data sets enables a direct network comparison [108].

A method to perform network comparison in the original network representation was recently proposed for the case of multichannel EEG by Crippa et al. [19]. This approach is based on representation of an EEG coherence network by a so-called *functional unit* (FU), which is defined as a spatially connected clique in the EEG graph, i.e., a set of electrodes used in the EEG experiment that are spatially close and record pairwise significantly coherent signals [92, 94]. To each electrode a Voronoi cell is associated and all cells belonging to an FU are given a corresponding color. Lines connect FU centers if the inter-FU coherence exceeds a significance threshold. The color of a line depends on the inter-FU coherence. Such a representation of the FUs in an EEG recording is called a FU map. FU maps can be constructed for different frequency bands or for different subjects (see Fig. 21.7).

Comparison of multiple FU maps can be done visually when displayed next to each other, but this method is limited as humans are notoriously weak in spotting visual differences in images. An alternative, which is more quantitative although it still involves visual assessment to a certain degree, is to compute a *mean* FU map, based upon the concept of *graph averaging* [19]. The mean of a set of input FU maps is defined in such a way that it not only represents the mean group coherence during a certain task or condition, but also to some extent displays individual variations in brain activity. The definition of a mean FU map relies on a graph dissimilarity measure that takes into account both node positions and node or edge attributes. A visualization of the mean FU map is used with a visual representation of the frequency of occurrence of nodes and edges in the input FUs. This makes it possible to investigate which brain regions are more commonly involved in a certain task, by analyzing the occurrence of an FU of the mean graph in the input FUs.

In [19] the graph averaging method was applied to the analysis of EEG coherence networks in two case studies, one on mental fatigue and one on patients with corticobasal ganglionic degeneration. An extension of the method to resting state fMRI data was presented in [18].

## 21.9 Conclusions

There is currently great scientific interest in connectomics, as it is believed to be an important prerequisite for understanding brain function. As much of the data for obtaining neural connectivity is image-based, visualization techniques are indispensable. Great effort has been put recently into extraction of connectivity information from images, integration of multimodal information into reference systems, and visual analysis of such data and systems at different scales. These efforts will need to be intensified in the future, as data is being produced at a much larger scale, also by new imaging modalities. New methods to integrate this data across modalities and scales to attain the ultimate goal, a description of the human connectome, will be the main challenge for visualization in connectomics.

## References

1. Appel, N.M.: Classical and contemporary histochemical approaches for evaluating central nervous system microanatomy. Ann. NY Acad. Sci. **820**(1), 14–28 (1997)
2. Basser, P.J., Pajevic, S., Pierpaoli, C., Duda, J., Aldroubi, A.: In vivo fiber tractography using DT-MRI data. Magn. Reson. Med. **44**(4), 625–632 (2000)
3. Bassett, D.S., Bullmore, E.: Small-world brain networks. Neuroscientist **12**(6), 512–523 (2006)
4. Behrens, T.E., Woolrich, M.W., Jenkinson, M., JohansenBerg, H., Nunes, R.G., Clare, S., Matthews, P.M., Brady, J.M., Smith, S.M.: Characterization and propagation of uncertainty in diffusion-weighted MR imaging. Magn. Reson. Med. **50**(5), 1077–1088 (2003)

5. Bertrand, L., Nissanov, J.: The neuroterrain 3D mouse brain atlas. Front. Neuroinform. **2**, 3 (2008)

6. Bezgin, G., Reid, A., Schubert, D., Kötter, R.: Matching spatial with ontological brain regions using java tools for visualization, database access, and integrated data analysis. Neuroinformatics **7**(1), 7–22 (2009)

7. Bjaalie, J.G.: Localization in the brain: new solutions emerging. Nat. Rev. Neurosci. **3**, 322–325 (2002)

8. Blaas, J., Botha, C.P., Peters, B., Vos, F.M., Post, F.H.: Fast and reproducible fiber bundle selection in DTI visualization. In: Silva, C., Gröller, E., Rushmeier, H. (eds.) Proceedings of IEEE Visualization 2005, pp. 59–64 (2005)

9. Bruckner, S., Gröller, M.: Instant volume visualization using maximum intensity difference accumulation. Comput. Graph. Forum **28**(3), 775–782 (2009)

10. Bullmore, E., Harrison, L., Lee, L., Mechelli, A., Friston, K.(eds.): Special issue on functional connectivity. Neuroinformatics **2**(2) (2004)

11. Bullmore, E., Sporns, O.: Complex brain networks: graph theoretical analysis of structural and functional systems. Nat. Rev. Neurosci. **10**, 186–198 (2009). see also Corrigendum (March 3, 2009)

12. Bullmore, E., Bassett, D.: Brain graphs: graphical models of the human brain connectome. Ann. Rev. Clin. Psychol. **7**, 113–140 (2011)

13. Burns, G.a.P.C., Cheng, W.C., Thompson, R.H., Swanson, L.W.: The NeuARt II system: A viewing tool for neuroanatomical data based on published neuroanatomical atlases. BMC Bioinform. **7**, 531–549 (2006)

14. Cardona, A., Saalfeld, S., Preibisch, S., Schmid, B., Cheng, A., Pulokas, J., Tomancak, P., Hartenstein, V.: An integrated micro- and macroarchitectural analysis of the drosophila brain by computer-assisted serial section electron microscopy. PLoS Biol **8**(10), e1000,502 (2010)

15. Chicurel, M.: Databasing the brain. Nature **406**(6798), 822–825 (2000)

16. Chklovskii, D.B., Vitaladevuni, S., Scheffer, L.K.: Semi-automated reconstruction of neural circuits using electron microscopy. Curr. Opin. Neurobiol. **20**(5), 667–675 (2010)

17. Conchello, J.A., Lichtman, J.: Optical sectioning microscopy. Nat. Methods **2**(12), 920–931 (2005)

18. Crippa, A., Roerdink, J.B.T.M.: Data-driven visualization of functional brain regions from resting state fMRI data. In: Eisert, P., Polthier, K., Hornegger, J. (eds.) Proceedings Vision, Modeling and Visualization Workshop (VMV), 4–6 Oct, Berlin, pp. 247–254 (2011)

19. Crippa, A., Maurits, N.M., Roerdink, J.B.T.M.: Graph averaging as a means to compare multichannel EEG coherence networks and its application to the study of mental fatigue and neurodegenerative disease. Comput. Graph. **35**(2), 265–274 (2011)

20. Da Costa, N.M., Fürsinger, D., Martin, K.A.C.: The synaptic organization of the claustral projection to the cat's visual cortex. J. Neurosci. **30**(39), 13,166–13,170 (2010)

21. Denk, W., Horstmann, H.: Serial block-face scanning electron microscopy to reconstruct three-dimensional tissue nanostructure. PLoS Biol. **2**(11), e329 (2004)

22. Dercksen, V.J., Oberlaender, M., Sakmann, B., Hege, H.C.: Interactive Visualization—a Key Prerequisite for Reconstruction of Anatomically Realistic Neural Networks. In: Linsen, L. (ed.) Visualization in Medicine and Life Sciences II. Springer, Berlin (2012)

23. Einstein, A.: Investigations on the Theory of the Brownian Movement. Dover (1956)

24. Emmenlauer, M., Ronneberger, O., Ponti, A., Schwarb, P., Griffa, A., Filippi, A., Nitschke, R., Driever, W., Burkhardt, H.: XuvTools: free, fast and reliable stitching of large 3D datasets. J. Microsc. **233**(1), 42–60 (2009)

25. Enders, F., Sauber, N., Merhof, D., Hastreiter, P., Nimsky, C., Stamminger, M.: Visualization of white matter tracts with wrapped streamlines. In: IEEE Visualization, 2005. VIS 05, pp. 51–58. IEEE (2005)

26. Everts, M.H., Bekker, H., Roerdink, J.B.T.M., Isenberg, T.: Depth-dependent halos: illustrative rendering of dense line data. IEEE Trans. Vis. Comput. Graph. **15**(6), 1299–1306 (2009)

27. Fair, D.A., Cohen, A.L., Power, J.D., Dosenbach, N.U.F., Church, J.A., Miezin, F.M., Schlaggar, B.L., Petersen, S.E.: Functional brain networks develop from a "local to distributed" organization. PLoS Comput. Biol. **5**(5), e1000,381 (2009)

28. Fair, D.A., Cohen, A.L., Dosenbach, N.U.F., Church, J.A., Miezin, F.M., Barch, D.M., Raichle, M.E., Petersen, S.E., Schlaggar, B.L.: The maturing architecture of the brain's default network. Proc. Natl. Acad. Sci. **105**(10), 4028–4032 (2008)

29. Fiala, J.C.: Reconstruct: a free editor for serial section microscopy. J. Microsc. **218**(1), 52–61 (2005)

30. Fornito, A., Zalesky, A., Pantelis, C., Bullmore, E.T.: Schizophrenia, neuroimaging and connectomics. NeuroImage **62**, 2296–2314 (2012)

31. Fredriksson, J.: Design of an Internet accessible visual human brain database system. In: Proceedings of IEEE International Conference on Multimedia Computing and Systems, vol. 1, pp. 469–474 (1999)

32. Friston, K.J.: Functional and effective connectivity in neuroimaging: a synthesis. Hum. Brain Mapp. **2**, 56–78 (1994)

33. Gan, W.B., Grutzendler, J., Wong, W.T., Wong, R.O.L., Lichtman, J.W.: Multicolor "DiOlistic" Labeling Neurotechnique of the Nervous System Using. Neuron **27**, 219–225 (2000)

34. Hagmann, P., Jonasson, L., Maeder, P., Thiran, J., Wedeen, V.J., Meuli, R.: Understanding diffusion MR imaging techniques: from scalar diffusion-weighted imaging to diffusion tensor imaging and beyond. Radiographics **26**(Suppl 1), S205–S223 (2006)

35. Hämäläinen, M., Hari, R., Ilmoniemi, R.J., Knuutila, J., Lounasmaa, O.V.: Magneto-encephalography—theory, instrumentation, and applications to noninvasive studies of the working human brain. Rev. Mod. Phys. **65**, 413–497 (1993)

36. Hayworth, K.J., Kasthuri, N., Schalek, R., Lichtman, J.W.: Automating the collection of ultrathin serial sections for large volume TEM reconstructions. Microsc. Microanal. **12**(S02), 86–87 (2006)

37. Helmstaedter, M., Briggman, K.L., Denk, W.: High-accuracy neurite reconstruction for high-throughput neuroanatomy. Nat. Neurosci. **14**, 1081–1088 (2011)

38. Huberman, A.D., Niell, C.M.: What can mice tell us about how vision works? Trends Neurosci. **34**(9), 464–473 (2011)

39. Jain, V., Bollmann, B., Richardson, M., Berger, D.R., Helmstaedter, M.N., Briggman, K.L., Denk, W., Bowden, J.B., Mendenhall, J.M., Abraham, W.C., Harris, K.M., Kasthuri, N., Hayworth, K.J., Schalek, R., Tapia, J.C., Lichtman, J.W., Seung, H.S.: Boundary learning by optimization with topological constraints. IEEE Conference on Computer Vision and Pattern Recognition pp. 2488–2495 (2010)

40. Jenett, A., Schindelin, J.E., Heisenberg, M.: The virtual insect brain protocol: creating and comparing standardized neuroanatomy. BMC Bioinform. **7**(1), 544–555 (2006)

41. Jeong, W.K., Johnson, M.K.: Display-aware Image Editing. IEEE International Conference on Computational Photography (2011)

42. Jeong, W.K., Beyer, J., Hadwiger, M., Blue, R., Law, C., Vazquez-Reina, A., Reid, R.C., Lichtman, J., Pfister, H.: Ssecrett and neurotrace: interactive visualization and analysis tools for large-scale neuroscience data sets. IEEE Comput. Graph. Appl. **30**(3), 58–70 (2010)

43. Joshi, S.H., Horn, J.D.V., Toga, A.W.: Interactive exploration of neuroanatomical meta-spaces. Front. Neuroinform. **3**, 38 (2009)

44. Jurrus, E., Paiva, A.R.C., Watanabe, S., Anderson, J.R., Jones, B.W., Whitaker, R.T., Jorgensen, E.M., Marc, R.E., Tasdizen, T.: Detection of neuron membranes in electron microscopy images using a serial neural network architecture. Med. Image Anal. **14**(6), 770–783 (2010)

45. Kaiser, M.: A tutorial in connectome analysis: Topological and spatial features of brain networks. NeuroImage **57**(3), 892–907 (2011) (Special Issue: Educational Neuroscience)

46. Kaynig, V., Fischer, B., Buhmann, J.M.: Probabilistic image registration and anomaly detection by nonlinear warping. In: IEEE Conference on Computer Vision and Pattern Recognition, pp. 1–8 (2008)

47. Kaynig, V., Fuchs, T., Buhmann, J.M.: Geometrical consistent 3D tracing of neuronal processes in ssTEM data. In: International Conference on Medical Image Computing and Computer Assisted Intervention (2010)

48. Kaynig, V., Fuchs, T., Buhmann, J.M.: Neuron geometry extraction by perceptual grouping in ssTEM images. In: T. Fuchs, J.M. Buhmann (eds.) IEEE Conference on Computer Vision and Pattern Recognition, pp. 2902–2909. IEEE (2010)

49. Kindlmann, G., Weinstein, D.: Hue-balls and lit-tensors for direct volume rendering of diffusion tensor fields. In: Proceedings of Visualization '99, pp. 183–524. IEEE (1999)

50. Kindlmann, G.: Superquadric tensor glyphs. In: Proceedings of IEEE TVCG/EG Symposium on Visualization, pp. 147–154 (2004)

51. Klein, J., Friman, O., Hadwiger, M., Preim, B., Ritter, F., Vilanova, A., Zachmann, G., Bartz, D.: Visual computing for medical diagnosis and treatment. Comput. Graph. **33**(4), 554–565 (2009)

52. Knott, G., Marchman, H., Wall, D., Lich, B.: Serial section scanning electron microscopy of adult brain tissue using focused ion beam milling. J. Neurosci. **28**(12), 2959–2964 (2008)

53. Koslow, S.H., Subramaniam, S.: Databasing the Brain: From Data to Knowledge. Wiley (2005)

54. Kötter, R.: Online retrieval, processing, and visualization of primate connectivity data from the cocomac database. Neuroinformatics **2**(2), 127–44 (2004)

55. Kuß, A., Prohaska, S., Meyer, B., Rybak, J., Hege, H.C.: Ontology-based visualization of hierarchical neuroanatomical structures. In: Proc. Eurographics Workshop on Visual Computing for Biomedicine, VCBM, Delft, The Netherlands, pp. 177–184 (2008)

56. Kuß, A., Gensel, M., Meyer, B., Dercksen, V., Prohaska, S.: Effective techniques to visualize filament-surface relationships. Comput. Graph. Forum **29**(3), 1003–1012 (2010)

57. Lang, S., Dercksen, V.J., Sakmann, B., Oberlaender, M.: Simulation of signal flow in three-dimensional reconstructions of an anatomically realistic neuronal network in rat vibrissal cortex. Neural Netw. **24**(9), 998–1011 (2011)

58. Lau, C., Ng, L., Thompson, C., Pathak, S., Kuan, L., Jones, A., Hawrylycz, M.: Exploration and visualization of gene expression with neuroanatomy in the adult mouse brain. BMC Bioinform. **9**, 153–163 (2008)

59. de Leeuw, W., Verschure, P.J., van Liere, R.: Visualization and analysis of large data collections: a case study applied to confocal microscopy data. IEEE Trans. Vis. Comput. Graph. **12**(5), 1251–1258 (2006)

60. Lichtman, J., Livet, J., Sanes, J.: A technicolour approach to the connectome. Nat. Rev. Neurosci. **9**(6), 417–422 (2008)

61. Lin, C.Y., Tsai, K.L., Wang, S.C., Hsieh, C.H., Chang, H.M., Chiang, A.S.: The Neuron Navigator: Exploring the information pathway through the neural maze. In: Proceedings of IEEE Pacific Visualization 2011, pp. 35–42. IEEE (2011)

62. Luscombe, N.M., Babu, M.M., Yu, H., Snyder, M., Teichmann, S.A., Gerstein, M.: Genomic analysis of regulatory network dynamics reveals large topological changes. Nature **431**, 308–312 (2004)

63. Mackay, T.F., Anholt, R.R.: Of flies and man: drosophila as a model for human complex traits. Ann. Rev. Genomics Hum. Genet. **7**, 339–367 (2006)

64. Maye, A., Wenckebach, T.H., Hege, H.C.: Visualization, reconstruction, and integration of neuronal structures in digital brain atlases. Int. J. Neurosci. **116**(4), 431–459 (2006)

65. Oberlaender, M., de Kock, C.P.J., Bruno, R.M., Ramirez, A., Meyer, H.S., Dercksen, V.J., Helmstaedter, M., Sakmann, B.: Cell Type-Specific Three-Dimensional Structure of Thalamocortical Circuits in a Column of Rat Vibrissal Cortex. Cerebral Cortex. **22**(10), 2375–2395 (2012) doi:10.1093/cercor/bhr317

66. Oberlaender, M., Dercksen, V.J., Egger, R., Gensel, M., Sakmann, B., Hege, H.C.: Automated three-dimensional detection and counting of neuron somata. J. Neurosci. Methods **180**(1), 147–160 (2009)

67. Ogawa, S., Lee, T.M., Kay, A.R., Tank, D.W.: Brain magnetic resonance imaging with contrast dependent on blood oxygenation. Proc. Natl. Acad. Sci. **87**(24), 9868–9872 (1990)

68. Ogawa, S., Tank, D.W., Menon, R., Ellermann, J.M., Kim, S.G., Merkle, H., Ugurbil, K.: Intrinsic signal changes accompanying sensory stimulation: functional brain mapping with magnetic resonance imaging. Proc. Natl. Acad. Sci. **89**(13), 5951–5955 (1992)

69. Özarslan, E., Mareci, T.H.: Generalized diffusion tensor imaging and analytical relationships between diffusion tensor imaging and high angular resolution diffusion imaging. Magn. Reson. Med. **50**(5), 955–965 (2003)

70. Peeters, T.H., Prčkovska, V., van Almsick, M., Vilanova, A., ter Haar Romeny, B.M.: Fast and sleek glyph rendering for interactive HARDI data exploration. In: Visualization Symposium, 2009. PacificVis '09. IEEE Pacific, pp. 153–160. IEEE (2009)

71. Pereanu, W., Hartenstein, V.: Neural lineages of the drosophila brain: a three-dimensional digital atlas of the pattern of lineage location and projection at the late larval stage. J. Neurosci. **26**(20), 5534–5553 (2006)

72. Perrin, M., Poupon, C., Cointepas, Y., Rieul, B., Golestani, N., Pallier, C., Rivire, D., Constantinesco, A., Bihan, D., Mangin, J.F.: Fiber tracking in q-Ball fields using regularized particle trajectories. In: Christensen, G.E., Sonka, M. (eds.) Inf. Process. Med. Imaging, vol. 3565, pp. 52–63. Springer, Berlin (2005)

73. Prčkovska, V., Peeters, T.H., van Almsick, M., ter, : Haar Romeny, B., Vilanova i Bartroli, A.: Fused DTI/HARDI visualization. IEEE Trans. Vis. Comput. Graph. **17**(10), 1407–1419 (2011)

74. Preibisch, S., Saalfeld, S., Tomancak, P.: Globally optimal stitching of tiled 3D microscopic image acquisitions. Bioinformatics **25**(11), 1463–1465 (2009)

75. Press, W.A., Olshausen, B.A., Essen, D.C.V.: A graphical anatomical database of neural connectivity. Philos. Trans. R. Soc. **356**(1412), 1147–1157 (2001)

76. Reina, A.V., Miller, E., Pfister, H.: Multiphase geometric couplings for the segmentation of neural processes. IEEE Conference on Computer Vision and Pattern Recognition, pp. 1–8 (2009)

77. Roberts, M., Jeong, W.K., V, A., Unger, M.: Neural Process Reconstruction from Sparse User Scribbles. In: Medical Image Computing and Computer Assisted Intervention, pp. 1–8 (2011)

78. Rubinov, M., Sporns, O.: Complex network measures of brain connectivity: Uses and interpretations. Neuroimage **52**, 1059–1069 (2010)

79. Rybak, J., Kuss, A., Lamecker, H., Zachow, S., Hege, H., Lienhard, M., Singer, J., Neubert, K., Menzel, R.: The digital bee brain: integrating and managing neurons in a common 3d reference system. Frontiers in systems neuroscience 4 (2010)

80. Salvador, R., Suckling, J., Coleman, M.R.: Pickard John, D., Menon, D., Bullmore, E.: Neurophysiological architecture of functional magnetic resonance images of human brain. Cereb Cortex **15**, 1332–1342 (2005)

81. Schomer, D.L., Lopes da Silva, F.: Niedermeyer's Electroencephalography: Basic Principles, Clinical Applications, and Related Fields. Wolters Kluwer/Lippincott Williams & Wilkins (2010)

82. Schultz, T., Theisel, H., Seidel, H.P.: Topological visualization of brain diffusion MRI data. IEEE Trans. Vis. Comput. Graph. **13**(6), 1496–1503 (2007)

83. Seung, S.: Connectome. Houghton Mifflin Harcourt (2011). In press

84. Sharan, R., Ideker, T.: Modeling cellular machinery through biological network comparison. Nat. Biotechnol. **24**(4), 427–433 (2006)

85. Sherbondy, A., Akers, D., Mackenzie, R., Dougherty, R., Wandell, B.: Exploring connectivity of the brain's white matter with dynamic queries. IEEE Trans. Vis. Comput. Graph. **11**(4), 419–430 (2005)

86. Shu, N., Liu, Y., Li, J., Li, Y., Yu, C., Jiang, T.: Altered anatomical network in early blindness revealed by diffusion tensor tractography. PLoS One **4**(9), e7228 (2009)

87. Sporns, O.: Networks of the brain. MIT Press, Cambridge (2010)

88. Sporns, O., Zwi, J.: The small world of the cerebral cortex. Neuroinformatics **2**, 145–162 (2004)

89. Sporns, O., Tononi, G., Kötter, R.: The human connectome: a structural description of the human brain. PLoS Comput. Biol. **1**(4), e42 (2005)

90. Stam, C.J., Reijneveld, J.C.: Graph theoretical analysis of complex networks in the brain. Nonlinear Biomed. Phys. **1** (2007)

91. Straehle, C., Köthe, U., Knott, G., Hamprecht, F.: Carving: Scalable Interactive Segmentation of Neural Volume Electron Microscopy Images. In: MICCAI, pp. 657–664 (2011)
92. Ten Caat, M., Maurits, N.M., Roerdink, J.B.T.M.: Functional unit maps for data-driven visualization of high-density EEG coherence. In: Proceedings of Eurographics/IEEE VGTC Symposium on Visualization (EuroVis), pp. 259–266 (2007)
93. Ten Caat, M.: Multichannel EEG visualization. Ph.D. thesis, Institute of Mathematics and Computing Science, University of Groningen, The Netherlands (2008)
94. Ten Caat, M., Maurits, N.M., Roerdink, J.B.T.M.: Data-driven visualization and group analysis of multichannel EEG coherence with functional units. IEEE Trans. Vis. Comput. Graph. **14**(4), 756–771 (2008)
95. Tuch, D.S., Reese, T.G., Wiegell, M.R., Makris, N., Belliveau, J.W., Wedeen, V.J.: High angular resolution diffusion imaging reveals intravoxel white matter fiber heterogeneity. Magn. Reson. Med. **48**(4), 577–582 (2002)
96. Tuch, D.S.: Qball imaging. Magn. Reson. Med. **52**(6), 1358–1372 (2004)
97. Türetken, E., González, G., Blum, C., Fua, P.: Automated reconstruction of dendritic and axonal trees by global optimization with geometric priors. Neuroinformatics **9**(2), 279–302 (2011)
98. Valiant, L.G.: A quantitative theory of neural computation. Biol. Cybern. **95**(3), 205–211 (2006)
99. Van Dixhoorn, A., Vissers, B., Ferrarini, L., Milles, J., Botha, C.P.: Visual analysis of integrated resting state functional brain connectivity and anatomy. In: Proc. Eurographics Workshop on Visual Computing for Biomedicine, VCBM, Leipzig, Germany, pp. 57–64 (2010)
100. Varshney, L.R., Chen, B.L., Paniagua, E., Hall, D.H., Chklovskii, D.B.: Structural properties of the caenorhabditis elegans neuronal network. PLoS Comput. Biol. **7**(2), 21 (2011)
101. Vazquez-Reina, A., Pfister, H., Miller, E.L.: Segmentation Fusion for Connectomics. International Conference on Computer Vision pp. 1–8 (2011)
102. Vilanova, A., Zhang, S., Kindlmann, G., Laidlaw, D.H.: An introduction to visualization of diffusion tensor imaging and its applications. In: Visualization and Image Processing of Tensor Fields. Springer (2005)
103. Vitaladevuni, S.N.: Co-clustering of image segments using convex optimization applied to em neuronal reconstruction. IEEE Conference on Computer Vision and Pattern Recognition pp. 2203–2210 (2010)
104. Walter, T., Shattuck, D.W., Baldock, R., Bastin, M.E., Carpenter, A.E., Duce, S., Ellenberg, J., Fraser, A., Hamilton, N., Pieper, S.: Ragan, M.a., Schneider, J.E., Tomancak, P., Hériché, J.K.: Visualization of image data from cells to organisms. Nat. Methods **7**(3s), S26–S41 (2010)
105. Wan, Y., Otsuna, H., Chien, C.B., Hansen, C.: An interactive visualization tool for multichannel confocal microscopy data in neurobiology research. IEEE Trans. Vis. Comput. Graph. **15**(6), 1489–1496 (2009)
106. White, J.G., Southgate, E., Thomson, J.N., Brenner, S.: The structure of the nervous system of the nematode caenorhabditis elegans. Philos. Trans. R. Soc. B Biol. Sci. **314**(1165), 1–340 (1986)
107. Worsley, K.J., Chen, J., Lerch, J., Evans, A.C.: Comparing functional connectivity via thresholding correlations and singular value decomposition. Philos. Trans. R. Soc. B Biol. Sci. **360**(1457), 913–920 (2005)
108. Zalesky, A., Fornito, A., Bullmore, E.T.: Network-based statistic: identifying differences in brain networks. Neuroimage **53**(4), 1197–1207 (2010)
109. Zhang, S., Demiralp, C., Laidlaw, D.H.: Visualizing diffusion tensor MR images using streamtubes and streamsurfaces. IEEE Trans. Vis. Comput. Graph. **9**(4), 454–462 (2003)